

Supplementary Information

Effects of Mg Doping on Remarkably Enhanced Electrochemistry Performances of $\text{Na}_3\text{V}_2(\text{PO}_4)_3$ Cathode Material for Sodium Ion Batteries

Hui Li,^a Xiqian Yu,^b Ying Bai,^{*a} Feng Wu,^a Chuan Wu,^{*a} Liang-Yu Liu^a and Xiao-Qing Yang^{*b}

^a Beijing Key Laboratory of Environmental Science and Engineering, School of Chemical Engineering and Environment, Beijing Institute of Technology, Beijing 100081, China.

^b Chemistry Department, Brookhaven National Laboratory, Upton, New York 11973, USA.

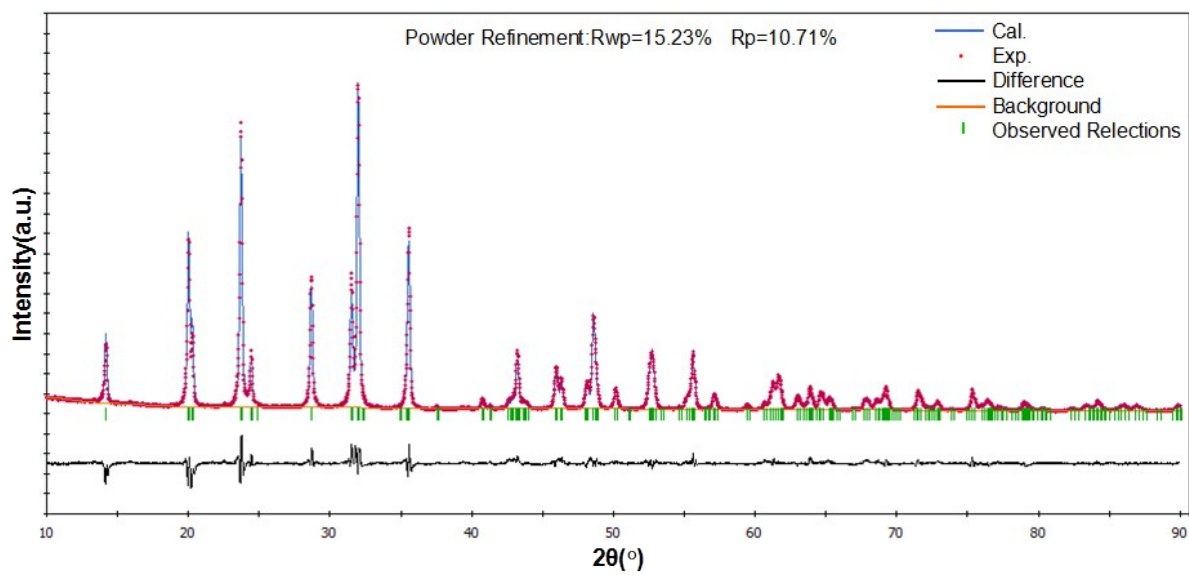


Fig. S1 Rietveld refined XRD patterns of $\text{Na}_3\text{V}_2(\text{PO}_4)_3$.

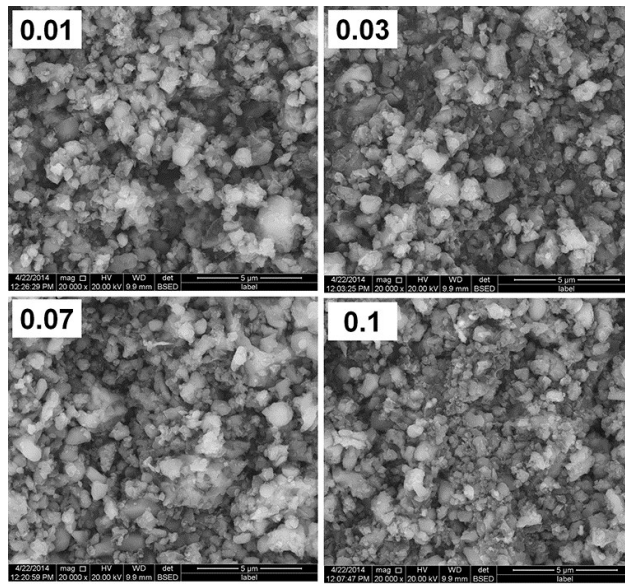


Fig. S2 SEM images of $\text{Na}_3\text{V}_{2-x}\text{Mg}_x(\text{PO}_4)_3$ ($x = 0.01, 0.03, 0.07$ and 0.1). As shown in Fig. S1, the particle of $\text{Na}_3\text{V}_{2-x}\text{Mg}_x(\text{PO}_4)_3$ ($x = 0.01, 0.03, 0.07$ and 0.1) is decreasing with the increasing x . The reduced particle sizes for $\text{Na}_3\text{V}_{2-x}\text{Mg}_x(\text{PO}_4)_3/\text{C}$ ($x=0.01, 0.03, 0.05, 0.07$ and 0.1) are attributed to the decomposition of $\text{Mg}(\text{CH}_3\text{COO})_2$ in the precursor mixtures, which prevents the agglomeration of final products during high temperature sintering. It is advantageous to enhance the electrochemical performance of the material, for the reduction of particle size will result in sufficient contact between active materials and electrolyte, which is favorable for shortening the distance of Na^+ diffusion and transmission. As a result, the $\text{Na}_3\text{V}_{2-x}\text{Mg}_x(\text{PO}_4)_3/\text{C}$ ($x=0.01, 0.03, 0.05, 0.07$ and 0.1) with smaller particle sizes would benefit in better electrochemical performance.

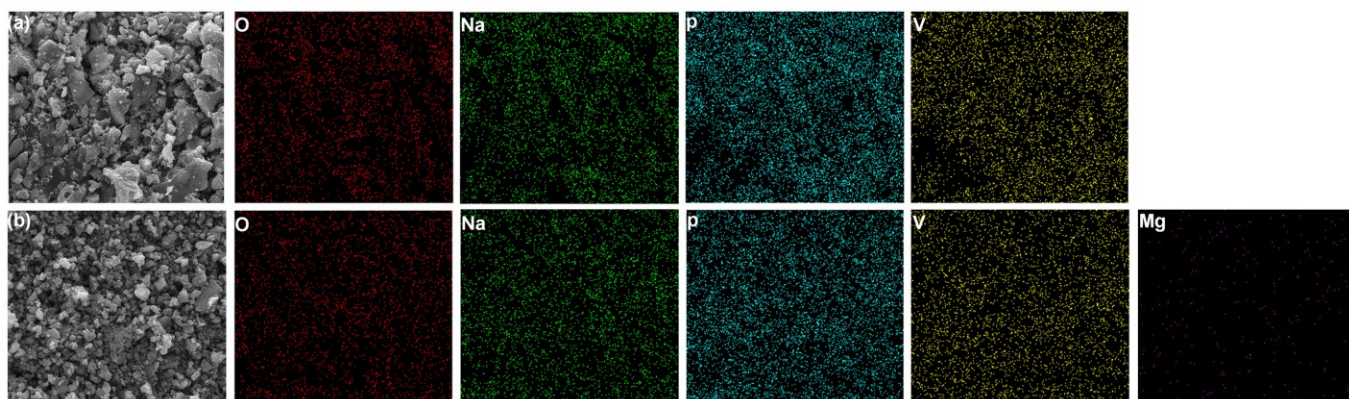


Fig. S3 EDS mapping images of a) $\text{Na}_3\text{V}_3(\text{PO}_4)_3$ and b) $\text{Na}_3\text{V}_{1.95}\text{Mg}_{0.05}(\text{PO}_4)_3$. Based on the EDX mapping images, it can be clearly observed that O, Na, V, P and Mg elements are uniformly distributed on the $\text{Na}_3\text{V}_{1.95}\text{Mg}_{0.05}(\text{PO}_4)_3$ particle.

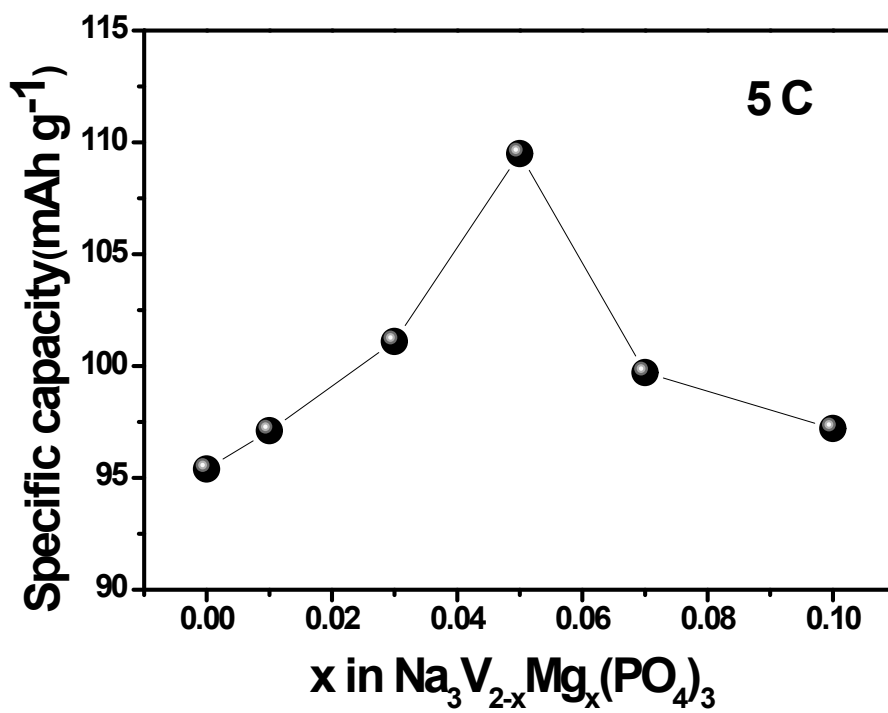


Fig. S4 The discharge capacities of Na₃V_{2-x}Mg_x(PO₄)₃/C(x=0, 0.01, 0.03, 0.05, 0.07 and 0.1) at 5 C. As shown in Fig. S2, with the increasing Mg doping content, the discharge capacities under the same current densities increase first, reach a maximum value when the x is 0.05 in Na₃V_{2-x}Mg_x(PO₄)₃/C, then decrease, displaying a volcano-type variation.

Table S1. XPS fitting parameters for V_{2p} signals in Na₃V_{1.95}Mg_{0.05}(PO₄)₃.

Element	Binding energy (eV)	FWHM (eV)	Area (eV cps)
V ³⁺ 2p	515.4	2.4	5637.327
V ⁴⁺ 2p	515.8	2.1	140.6294

From the fitting results, the areas obtained for the V³⁺ 2p and V⁴⁺ 2p peaks can be used to calculate the approximate concentration ratio of V³⁺ and V⁴⁺, according to the following equation:

$$\frac{N_{V^{3+}}}{N_{V^{4+}}} = \frac{I_{V^{3+}}}{I_{V^{4+}}}$$

where $I_{V^{3+}}$ and $I_{V^{4+}}$ represent the areas of the V³⁺ 2p and V⁴⁺ 2p peaks under their curves. The concentration ratio of 40 for V³⁺ to V⁴⁺ in Na₃V_{1.95}Mg_{0.05}(PO₄)₃ sample is calculated based on the above equation, which is close to the values of 39 (=1.95/0.05) obtained from the stoichiometric ratio. Therefore, it is reasonable to further assume that both the V³⁺ and V⁴⁺ ion coexist in Mg doped Na₃V₂(PO₄)₃ and magnesium is successfully substituted for vanadium.

Table S2. Results of structural analysis obtained from XRD Rietveld refinement of samples $\text{Na}_3\text{V}_2(\text{PO}_4)_3$ and $\text{Na}_3\text{V}_{1.95}\text{Mg}_{0.05}(\text{PO}_4)_3$

Samples	Lattice constant/Å			Lattice bond/Å			Reliability factors/%	
	a(=b)	c	v	V-O average	P-O average	Na-O average	R_{wp}	R_p
$\text{Na}_3\text{V}_2(\text{PO}_4)_3$	8.6853	21.6859	1416.71	2.018	1.529	2.819	15.23	10.71
$\text{Na}_3\text{V}_{1.95}\text{Mg}_{0.05}(\text{PO}_4)_3$	8.6757	21.6673	1412.37	2.016	1.527	2.822	13.08	9.88

Table S3. Crystallographic data of the $\text{Na}_3\text{V}_2(\text{PO}_4)_3$

Atom	Type	X/a	Y/b	Z/c	Occupancy
O1	O	0.14193	0.49765	0.07762	1.00
O2	O	0.54047	0.84480	-0.02643	1.00
V	V	0.33333	0.66667	0.01950	1.00
Na1	Na	0.33333	0.66667	0.16667	0.81
Na2	Na	0.66667	0.96724	0.08333	0.73
P	P	-0.04271	0.33333	0.08333	1.00

Table S4. Crystallographic data of the $\text{Na}_3\text{V}_{1.95}\text{Mg}_{0.05}(\text{PO}_4)_3$

Atom	Type	X/a	Y/b	Z/c	Occupancy
O1	O	0.14193	0.49765	0.07762	1.00
O2	O	0.54047	0.84480	-0.02643	1.00
V	V	0.33333	0.66667	0.01950	0.975
Mg	Mg	0.33333	0.66667	0.01950	0.025
Na1	Na	0.33333	0.66667	0.16667	0.81
Na2	Na	0.66667	0.96724	0.08333	0.73
P	P	-0.04271	0.33333	0.08333	1.00

Table S5. Molar ratio of the Mg²⁺ doping Na₃V_{2-x}Mg_x(PO₄)₃/C(x=0, 0.01, 0.03, 0.05, 0.07 and 0.1) samples determined using ICP-OES

Samples	x=0	x=0.01	x=0.03	x=0.05	x=0.07	x=0.1
Na:V:Mg(theoretical)	3:2	3:1.99:0.01	3:1.97:0.03	3:1.95:0.05	3:1.93:0.07	3:1.9:0.1
Na:V:Mg(experimental)	2.92:2	2.95:1.99:0.010	2.93:1.97:0.033	2.97:1.95:0.052	2.95:1.93:0.074	2.96:1.9:0.102

Table S6. The rate performances of $\text{Na}_3\text{V}_2(\text{PO}_4)_3$ cathode materials in sodium ion batteries

	This work	Ref. 1	Ref. 2	Ref.3	Ref.4	Ref.5	Ref.6
Cathode material	$\text{Na}_3\text{V}_{1.95}\text{Mg}_{0.05}(\text{PO}_4)_3$	$\text{Na}_3\text{V}_2(\text{PO}_4)_3$	$\text{Na}_3\text{V}_2(\text{PO}_4)_3$	$\text{Na}_3\text{V}_2(\text{PO}_4)_3$	$\text{Na}_3\text{V}_2(\text{PO}_4)_3$	$\text{Na}_3\text{V}_2(\text{PO}_4)_3$	$\text{Na}_3\text{V}_2(\text{PO}_4)_3$
1C(mA g ⁻¹)	117.6	117.5	110	117.6	118	117.6	117
Electrolyte	NaPF ₆	NaClO ₄	NaClO ₄	NaClO ₄	NaClO ₄	NaClO ₄	NaClO ₄
Solvent	EC/DEC	EC/PC	EC/DEC	EC/DMC	EC/DEC	PC	PC
Potential window(V)	2.5-4.0	2.3-3.9	2.7-4.0	2.3-3.9	2.7-4.0	2.5-3.8	2.5-3.8
Low rate capacity (mA h g ⁻¹)	112.5	114	118	117.5	102	93	77
	(1 C)	(1 C)	(0.05 C)	(0.5 C)	(0.2 C)	(1 C)	(2 C)
High rate capacity (mA h g ⁻¹)	94.2	61	90	97	84.3	58.79	20
	(30 C)	(40 C)	(5 C)	(5 C)	(5 C)	(30 C)	(20 C)
Capacity retention	83.7%	54%	76%	82.5%	82.6%	63.2%	25.9%

Our $\text{Na}_3\text{V}_{1.95}\text{Mg}_{0.05}(\text{PO}_4)_3/\text{C}$ shows remarkably improved rate capability and delivers a discharge capacity as high as 112.5, 111.3, 109.9, 108.5, 103.9 and 94.2 mAh g⁻¹ at 1, 2, 5, 10, 20 and 30 C. Such excellent rate capability is also quite impressive when compared to the reported values in the literature. When the electrode material is charged/discharged at small current density (~1 C), the capacity of our $\text{Na}_3\text{V}_{1.95}\text{Mg}_{0.05}(\text{PO}_4)_3/\text{C}$ is a little higher than most the reported work. However, when the electrode material is charged/discharged at high current density, our $\text{Na}_3\text{V}_{1.95}\text{Mg}_{0.05}(\text{PO}_4)_3/\text{C}$ displays remarkably enhanced electrochemical performance. For example, the capacity of our $\text{Na}_3\text{V}_{1.95}\text{Mg}_{0.05}(\text{PO}_4)_3/\text{C}$ at 30 C is far higher than Ref. 6 at 20 C with 20 mAh g⁻¹, Ref. 5 at 30 C with 58.79 mAh g⁻¹ and Ref. 4 at 5 C with 84.3 mAh g⁻¹. Therefore, Mg doping is an effective way to enhance the rate performance of $\text{Na}_3\text{V}_2(\text{PO}_4)_3$.

Table S7. Kinetic parameters of $\text{Na}_3\text{V}_{2-x}\text{Mg}_x(\text{PO}_4)_3/\text{C}$ ($x=0, 0.01, 0.03, 0.05, 0.07$ and 0.1) obtained from equivalent circuit fitting

x in $\text{Na}_3\text{V}_{2-x}\text{Mg}_x(\text{PO}_4)_3$	$\text{Re}(\Omega)$	$\text{Rct}(\Omega)$
0	5.597	967.7
0.01	6.402	335.2
0.03	4.406	240.3
0.05	2.49	226.1
0.07	3.866	456.4
0.1	7.657	601.8

Reference

- [1] K. Saravanan, C. W. Mason, A. Rudola, K. H. Wong and P. Balaya, *Adv. Energy Mater.*, 2013, 3, 444.
- [2] W. Shen, C. Wang, H. M. Liu and W. S. Yang, *Chem.Eur. J.*, 2013, 19, 14712.
- [3] S. Li, Y. F. Dong, L. Xu, X. Xu, L. He and L. Q. Mai, *Adv. Mater.*, 2014, 26, 3545.
- [4] W. Shen, C. Wang, Q. J. Xu, H. M. Liu and Y. G. Wang, *Adv. Energy Mater.*, 2014, 1400982. 5
- [5] G. Q. Li, D. L. Jiang, H. Wang, X. Z. Lan, H. H. Zhong and Y. Jiang, *J. Power Sources*, 2014, 265, 325.
- [6] J. Liu, K. Tang, K. P. Song, P. A. V. Aken, Y. Yu and J. Maier, *Nanoscale*, 2014, 6, 5081.